EPJ Web of Conferences **60**, 20045 (2013)
DOI: 10.1051/epjconf/20136020045

Search for the Standard Model Higgs boson in $H \to \mu^+\mu^-$ decays with the ATLAS detector

Christian Rudolph[1,a] on behalf of the ATLAS Collaboration

[1] *Technische Universität Dresden*

Abstract. An inclusive search for the Standard Model Higgs boson in the dimuon decay channel is presented. The search utilizes 20.7 fb^{-1} of proton-proton collision data at a center-of-mass energy of $\sqrt{s}$ = 8 TeV recorded by the ATLAS detector in 2012. No evidence of a signal is seen, therefore upper limits are set on $\sigma(pp \to H + X) \times \Gamma(H \to \mu^+\mu^-)$ as a function of the Higgs boson mass.The observed (expected) limit at the 95 % CL for the Higgs boson with a mass of 125 GeV is 9.8 (8.2) times the Standard Model prediction.

1 Introduction

The success of the Standard Model (SM) in the description and prediction of particle physics phenomena reached a climax in summer 2012, where both the ATLAS [1] and CMS [11] collaborations reported the discovery of a Higgs boson with a mass of approximately 125 GeV [2, 3]. Three experimentally accessible fermionic decay channels of the Higgs boson are present to investigate the Yukawa couplings: $H \to b\bar{b}$, $H \to \tau^+\tau^-$ and $H \to \mu^+\mu^-$. The latter provides a clean and fully reconstructible final state, but with a small branching ratio (28×10^{-5} to 6×10^{-5}, for a Higgs mass range of 110 – 150 GeV) and the dominant irreducible background from the $Z/\gamma^* \to \mu^+\mu^-$ process.

This document presents an inclusive search for the SM $H \to \mu^+\mu^-$ process in the dimuon invariant mass range from 110 – 150 GeV.

2 Data and simulated samples

The search is carried out on a data sample recorded by the ATLAS detector at $\sqrt{s}$ = 8 TeV. A single muon trigger is required with a transverse momentum threshold of p_{T} = 24 GeV. With this trigger and after application of data quality requirements the total integrated luminosity of the data sample is 20.7 ± 0.7 fb^{-1}.

Signal Monte-Carlo (MC) simulated event samples are generated for the gluon fusion (*ggF*), vector boson fusion (*VBF*) and vector-boson associated (*VH*) Higgs production channels, each in steps of 5 GeV in the Higgs mass, ranging from 110 – 150 GeV. The *ggF* and *VBF* samples are generated with Powheg [4] using the CT10nlo [13] parton distribution function (PDF), interfaced to Pythia8 [5]. The latter is the sole generator for the *VH* samples.

Background MC samples used in this analysis include $Z/\gamma^* + jets$, $W + jets$, diboson samples and events containing at least one top-quark. Both the signal and background samples are processed through a full Geant4 [7] ATLAS detector simulation, followed by the same reconstruction algorithms as used for collision data events.

The background MC samples are used to derive an analytical background function, whose overall normalization and shape parameters are measured directly from data signal regions (as discussed in Section 4.1).

3 Event selection

The $H \to \mu^+\mu^-$ candidate events are selected by requiring exactly two oppositely charged muons reconstructed both in the inner detector and in the muon spectrometer (*combined muons*). The leading muon has to have a transverse momentum of $p_{\mathrm{T}} > 25$ GeV, matched to the fired muon trigger within a spatial distance of $\Delta R < 0.15^{\dagger}$, whereas the subleading muon has to fulfill $p_{\mathrm{T}} > 15$ GeV. Both muons are restricted to $|\eta| < 2.5$, and are required to fulfill both track and calorimeter isolation criteria that scale with the muons' transverse momenta. To further suppress Drell-Yan background, the dimuon transverse momentum $p_{\mathrm{T}}^{\mu_1\mu_2}$ has to be larger than 15 GeV. A control region is defined by inverting this requirement.

To increase the sensitivity, the selected events are further separated in two resolution categories: if $|\eta_{\mu_{1,2}}| < 1$, the event falls into the central category; if one or both muons fail this criterion, the event is called non-central.

The signal region is defined via the invariant mass $m_{\mu\mu}$ of the dimuon system: 105 GeV $< m_{\mu\mu} <$ 160 GeV, extending the 110 – 150 GeV search window to account for the finite signal width. A data – MC comparison plot of the dimuon invariant mass before applying the signal search window is shown in Fig. 1.

[a] e-mail: c.rudolph@physik.tu-dresden.de

[†] The cone ΔR is defined as $\Delta R = \sqrt{(\Delta\eta)^2 + (\Delta\phi)^2}$, with η being the pseudorapidity and ϕ the radial angle in the $x - y$ plane.

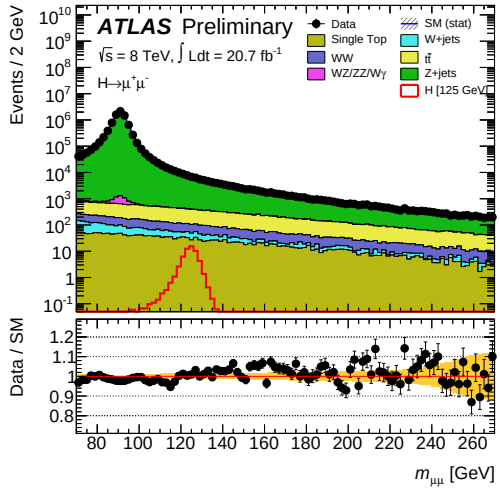

Figure 1. The dimuon invariant mass distribution before applying the invariant mass signal window and the resolution categories. The lower part of each plot shows the ratio between the data and the background expectation from MC, with the yellow band indicating the statistical uncertainty in the normalization of the various components. The signal is shown for $m_H = 125$ GeV [6].

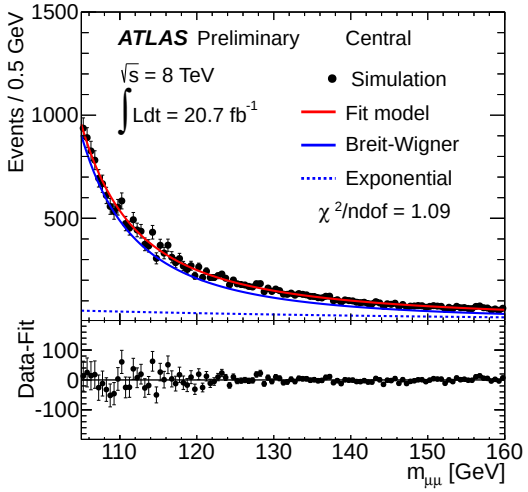

Figure 2. The background pdf fit performance in the central category on simulated MC background sample. The lower part of the plot shows the difference between simulated data points and the fit result [6].

4 Signal and background modeling

The results are derived via a binned maximum likelihood fit to the dimuon mass distributions in the central and non-central categories, using the sum of signal and background probability density functions (pdf).

4.1 Background model

The background pdf is inspired by the Z^0 lineshape and incorporates the sum of a Breit-Wigner (BW) and exponential pdf:

$$P_{BG}(x) = f_{BW} \cdot BW\,(x, M_Z, \Gamma_Z) + (1 - f_{BW}) \cdot P(e^{B \cdot x}),$$

with x being the the invariant dimuon mass and f_{BW} representing the BW fraction contribution after normalization to unity. M_Z and Γ_Z are both fixed to the world average values for the mass and width of the Z^0 boson [8]. The fit performance has been tested for both resolution categories on both background MC simulated samples and the data control region defined in Section 3. Figure 2 shows the performance of the background pdf fit on the MC simulated background sample for the central resolution category.

4.2 Signal model

The signal pdf is parametrized as the sum of a Crystal Ball [12] (CB) pdf and a Gaussian (GS) pdf:

$$P_S(x) = f_{CB} \cdot CB(x, m, \sigma_{CB}, \alpha, n) + (1 - f_{CB}) \cdot GS\,(x, m, \sigma_G)\,,$$

with x representing the dimuon mass and f_{CB} the fraction of the CB. This fraction is fixed to $f_{CB} = 0.9$ in the fit. Figure 3 shows the fit result of the signal pdf on the 125 GeV

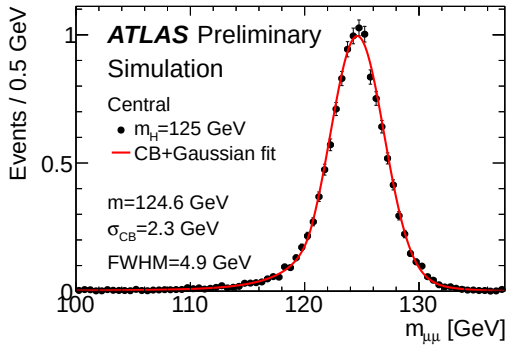

Figure 3. The signal pdf fit performance in the central category on simulated MC signal sample for $m_H = 125$ GeV. [6]

Higgs signal MC sample for the central resolution category. The remaining free parameters σ_{CB}, σ_{GS} and m of the fit are interpolated linearly between Higgs masses in steps of 0.5 GeV.

5 Systematic uncertainties

The expected signal yield is affected by uncertainties on the Higgs production cross-section ($\approx$ 15 % for ggF), the uncertainty on the branching ratio $\Gamma(H \rightarrow \mu^+\mu^-)$ ($\approx$ 6 % for $m_H = 125$ GeV) and uncertainties on the signal acceptance after analysis cuts. The latter are evaluated by varying the nominal generator setup for initial and final state radiation, and renormalization and factorization scales within their respective uncertainties. The effect of uncertainties on the PDF was investigated by using each of the CT10nlo [13] error PDFs in the simulation and comparing to the nominal setup. These variations resulted in relative acceptance uncertainties of 1 – 4 %, depending on the resolution category.

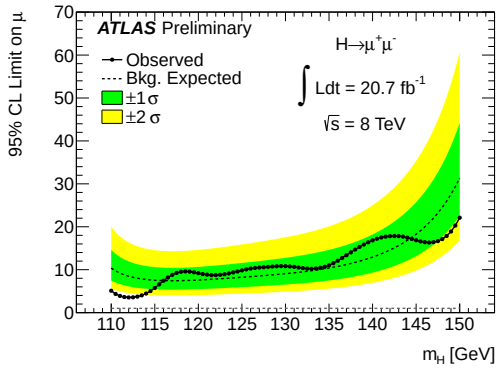

Figure 4. Expected and observed 95 % CL limits on the signal strength μ as a function of the Higgs mass in the range 110 – 150 GeV. The green (yellow) bands indicate the $\pm 1\sigma$ ($\pm 2\sigma$) uncertainty on the expected limits including all systematic uncertainties. [6]

The main source of experimental systematic uncertainty stems from the luminosity measurement, which has an uncertainty of 3.6 % [14]. The muon selection efficiency has an uncertainty of 0.3 – 1 % as a function of p_{T} and η. Other experimental systematic uncertainties include the muon momentum scale and resolution, muon trigger, muon isolation and pile-up interaction modeling, all of which were found to be less than 1 %.

6 Results and conclusions

The dimuon invariant mass distribution is fitted with a binned maximum likelihood fit using the sum of signal and background pdfs, simultaneously in the two resolution categories. No evidence of a narrow signal peak is observed.

Therefore upper limits are computed on the signal strength parameter μ, acting as a scale factor for the total number of events predicted by the SM for the $H \to \mu^+\mu^-$ signal, where $\mu = 0$ corresponds to the background-only hypothesis and $\mu = 1$ is identified as the SM $H \to \mu^+\mu^-$ signal in addition to the background. The limit is obtained using a modified frequentist CL_S method [9, 10]. The observed (expected) 95 % CL limits range between 3.5 (7.4) and 22.1 (31.3) times the SM prediction in the mass range 110 – 150 GeV. The expected and observed 95 % CL limits in the investigated mass range are shown in Fig. 4.

To conclude, an inclusive search for the SM Higgs boson in $H \to \mu^+\mu^-$ decays in proton-proton collisions at $\sqrt{s} = 8$ TeV at the ATLAS experiment has been carried out. In absence of an evidence for a signal, upper limits are set as a function of the Higgs boson mass. The observed (expected) 95 % CL limit for the Higgs boson with a mass of 125 GeV is 9.8 (8.2) times the SM prediction.

References

[1] ATLAS Collaboration, JINST **3** S08003 (2008)
[2] ATLAS Collaboration, Phys.Lett. **B716**, 1–29 (2012)
[3] CMS Collaboration, Phys.Lett. **B716**, 30–61 (2012)
[4] C. Oleari, Nucl.Phys.Proc.Suppl. **205-206**, 36–41 (2010)
[5] T. Sjostrand, Comp.Phys.Com. **178**, 852–867 (2008)
[6] ATLAS Collaboration, ATLAS-CONF-2013-010 (2013), `http://cdsweb.cern.ch/record/1523695`
[7] S. Agostinelli *et al.*, Nucl.Instrum.Meth. **A506**, 250 (2003)
[8] J.Beringer *et al.*, Phys.Rev. **D86**, (2012)
[9] G. Cowen *et al.*, EPJ **C71**, 1554 (2011)
[10] A. L. Read, J.Phys. **G28**, 2693–2704 (2002)
[11] CMS Collaboration, JINST **3** S08004 (2008)
[12] J. Gaiser, SLAC-R-0255 (1982)
[13] H.-L. Lai *et al.*, Phys.Rev **D82** 074024 (2010)
[14] ATLAS Collaboration, CERN-PH-EP-2013-026 (2013)